AGU PUBLICATIONS

JGR

Journal of Geophysical Research: Biogeosciences

RESEARCH ARTICLE
10.1002/2014JG002635

**Key Points:**
- Woody encroachment changes ecosystem structure and function
- Fluvial erosion increases following woody encroachment
- Results in increased losses of previously protected organic carbon

**Correspondence to:**
A. Puttock,
ap267@exeter.ac.uk

**Citation:**
Puttock, A., J. A. J. Dungait, C. J. A. Macleod, R. Bol, and R. E. Brazier (2014), Woody plant encroachment into grasslands leads to accelerated erosion of previously stable organic carbon from dryland soils, *J. Geophys. Res. Biogeosci.*, *119*, 2345–2357, doi:10.1002/2014JG002635.

Received 31 JAN 2014
Accepted 16 NOV 2014
Published online 30 DEC 2014

# Woody plant encroachment into grasslands leads to accelerated erosion of previously stable organic carbon from dryland soils

**Alan Puttock[1], Jennifer A. J. Dungait[2], Christopher J. A. Macleod[3], Roland Bol[4], and Richard E. Brazier[1]**

[1]Geography, College of Life and Environmental Sciences, University of Exeter, Exeter, UK, [2]Sustainable Systems and Grasslands Soils Department, Rothamsted Research North Wyke, Okehampton, UK, [3]The James Hutton Institute, Aberdeen, UK, [4]Institute of Bio- and Geosciences, Agrosphere, Forschungszentrum Jülich GmbH, Jülich, Germany

**Abstract** Drylands worldwide are experiencing rapid and extensive environmental change, concomitant with the encroachment of woody vegetation into grasslands. Woody encroachment leads to changes in both the structure and function of dryland ecosystems and has been shown to result in accelerated soil erosion and loss of soil nutrients. Covering 40% of the terrestrial land surface, dryland environments are of global importance, both as a habitat and a soil carbon store. Relationships between environmental change, soil erosion, and the carbon cycle are uncertain. There is a clear need to further our understanding of dryland vegetation change and impacts on carbon dynamics. Here two grass-to-woody ecotones that occur across large areas of the southwestern United States are investigated. This study takes a multidisciplinary approach, combining ecohydrological monitoring of structure and function and a dual-proxy biogeochemical tracing approach using the unique natural biochemical signatures of the vegetation. Results show that following woody encroachment, not only do these drylands lose significantly more soil and organic carbon via erosion but that this includes significant amounts of legacy organic carbon which would previously have been stable under grass cover. Results suggest that these dryland soils may not act as a stable organic carbon pool, following encroachment and that accelerated erosion of carbon, driven by vegetation change, has important implications for carbon dynamics.

## 1. Introduction

Drylands cover over 40% of the terrestrial land surface, constituting the largest biome on the planet [*Schimel*, 2010] and are home to 2.3 billion people [*World Resources Institute*, 2002]. Due to the combined pressures of climate change and demography, both the area and human population of drylands will continue to increase [*Reynolds et al.*, 2007; *Seager et al.*, 2007]. Over half of the current dryland population relies directly on the land, is classified as socioeconomically marginalized, and thus, is particularly vulnerable to environmental change [*Zafar et al.*, 2005]. Many drylands globally, including large areas of the southwestern United States (southwestern U.S.), have recently experienced, or are currently undergoing, extensive environmental change, driven by the encroachment of woody vegetation into grasslands [*King et al.*, 2012; *Zafar et al.*, 2005]. In the U.S., lands undergoing encroachment are estimated to cover $330 \times 10^6$ ha [*Eldridge et al.*, 2011; *Knapp et al.*, 2008]. Observations from the grass-woody vegetation transitions occurring in drylands across the southwestern U.S. suggest that the competitive ability of grass species is being reduced, allowing woody species to encroach and that ecosystems are adjusting to a change in current or historic controls on vegetation patterns [*Archer*, 1995]. Cited drivers of woody encroachment include climate [*Seager et al.*, 2007], atmospheric $CO_2$ [*Higgins and Scheiter*, 2012], fire [*Yu and D'Odorico*, 2014], and animal activity, particularly grazing [*Van Auken*, 2009], and it is generally recognized that encroachment results from a combination of both climatic and land use drivers [*Peters et al.*, 2013].

Dryland soils represent an important global carbon (C) pool [*Campbell et al.*, 2008; *Eswaran et al.*, 2000] and store over a quarter of global soil organic carbon (SOC) [*Zafar et al.*, 2005]; in North America, dryland SOC constitutes an estimated 121 Gt of a total of 388 Gt [*Campbell et al.*, 2008]. Research has shown that C storage in areas dominated by woody vegetation can be higher than grass, both in terms of plant biomass [*Fang et al.*, 2001] and SOC as a result of greater aggregate stability and biomass inputs [*Bird et al.*, 2002]. Thus, it has been suggested that woody encroachment into grasslands could increase the C sequestration potential of

landscapes [*Barger et al.*, 2011; *Hurtt et al.*, 2002; *Jobbagy and Jackson*, 2000]. However, woody encroachment in drylands alters ecosystem structure and function [*Barger et al.*, 2011; *Turnbull et al.*, 2008a], potentially leading to degradation [*Okin et al.*, 2009; *D'Odorico et al.*, 2013]. The change in structure, following encroachment, is often characterized by a reduction in vegetation cover [*Turnbull et al.*, 2010a] and increased heterogeneity in both soil and vegetation resources [*Dickie and Parsons*, 2012; *Bhark and Small*, 2003]. The "island of fertility" effect [*Schlesinger et al.*, 1990] leads to the trapping and storage of resources under vegetated patches [*Ridolfi et al.*, 2008] and loss of resources from bare areas exhibiting lower erosion thresholds [*Pierson et al.*, 2010; *Wainwright et al.*, 2011]. Vegetation patch dynamics are therefore a key control on overland flow [*Archer et al.*, 2011], and together, the strong interactions between ecological and hydrological processes create a self-reinforcing heterogeneous structure [*Schlesinger et al.*, 1990].

Soil erosion is the most common global cause of soil degradation [*Olderman*, 1994], leading to reduced soil fertility [*Schlesinger et al.*, 1990], sedimentation, and water quality issues in receiving surface waters [*Mukundan et al.*, 2012]. Being concentrated in fine surface soil and of low density, SOC is preferentially removed by fluvial erosion [*Lal*, 2005]. Soil erosion alters soil-atmosphere C fluxes via three key mechanisms [*Van Oost et al.*, 2007] including (1) replacement of eroded SOC by plant input, (2) deep burial limiting decomposition, and (3) enhanced decomposition due to the processes involved in detaching and transporting SOC. However, the balance between these mechanisms and the exact role played by soil erosion in the global C cycle are a major source of uncertainty [*Jackson et al.*, 2002; *Lal*, 2005; *Van Oost et al.*, 2007; *Berhe and Kleber*, 2013]. Further research is required to develop techniques that can aid in the identification and accounting for the source of eroded C [*Nadeu et al.*, 2012]. Therefore, with the identified importance and uncertainty regarding C dynamics in dryland systems [*Poulter et al.*, 2014; *Barger et al.*, 2011], it is crucial to quantify the impact of erosion processes that are accelerated by woody encroachment on SOC dynamics in these landscapes [*Brazier et al.*, 2013; *Breshears et al.*, 1999].

Biogeochemical techniques have been developed which utilize the unique signatures of plants to differentiate between sources of SOC. Dryland grass species that use $C_4$ photosynthesis (Hatch–Slack pathway) have different natural abundant stable C isotope signatures ($\delta^{13}C$ values) relative to that of the woody species (that use $C_3$ photosynthesis) encroaching into dryland grasslands in the southwestern U.S. [*Mendez-Millan et al.*, 2013; *Zech et al.*, 2009]. The $\delta^{13}C$ values have previously been used to develop understanding of erosional processes [*Nadeu et al.*, 2012] including their ability to differentiate between SOC derived from $C_3$ or $C_4$ sources in southwestern U.S. drylands [*Puttock et al.*, 2012]. Additionally, the compound-specific signatures of long-chain *n*-alkanes (aliphatic hydrocarbons) from leaf waxes have been used to differentiate between inputs from woody or grassland species into soils [*Eglinton et al.*, 1962; *Jansen et al.*, 2006]. It has been shown that large amounts of *n*-alkanes with a hydrocarbon chain length of 31 ($C_{31}$) often indicate a grass source [*Eckmeier and Wiesenberg*, 2009], while the shorter $C_{27}$ is commonly indicative of a woody source [*Zech et al.*, 2009]. Therefore, the ratio between $C_{27}$ and $C_{31}$ offers a means by which to trace source and movement of SOC and associated sediment. Both techniques use natural products of plants growing in ecosystems and offer economic and practical advantages over techniques using applied synthetic tracers [*Divine and McDonnell*, 2005].

Herein, we employ a dual-proxy approach, utilizing both the bulk $\delta^{13}C$ values and *n*-alkane signatures of dryland plants, to infer the sources of organic C in soils and fluvially eroded sediments across two dryland ecotones where woody species encroach neighboring grasslands. Biogeochemical analysis is combined with the ecohydrological monitoring of vegetation and soil structure, in addition to hydrological function across the monitored ecotones, to quantify the spatial distribution of organic C and losses via fluvial erosion.

## 2. Study Sites

Four sites (grama grassland in basin site, creosote shrubland site, grama grassland at Los Piños site, and piñon-juniper woodland site) were used to monitor ecosystem structure and attendant hydrological function [*Puttock et al.*, 2013] over grassland-to-shrubland and grassland-to-woodland ecotones (Figure 1). Sites were located in the Sevilleta National Wildlife Refuge (SNWR), New Mexico, USA (34°19′N, 106°42′W), which lies across the Rio Grande rift valley. At the SNWR (Figure 1), the study area is underlain by Quaternary, sedimentary geology of the Santa Fe Group [*Rawling*, 2004]. The study sites were located upon well drained, moderately permeable gravelly sandy loams. In the Rio Grande basin, the study sites (grama grassland in

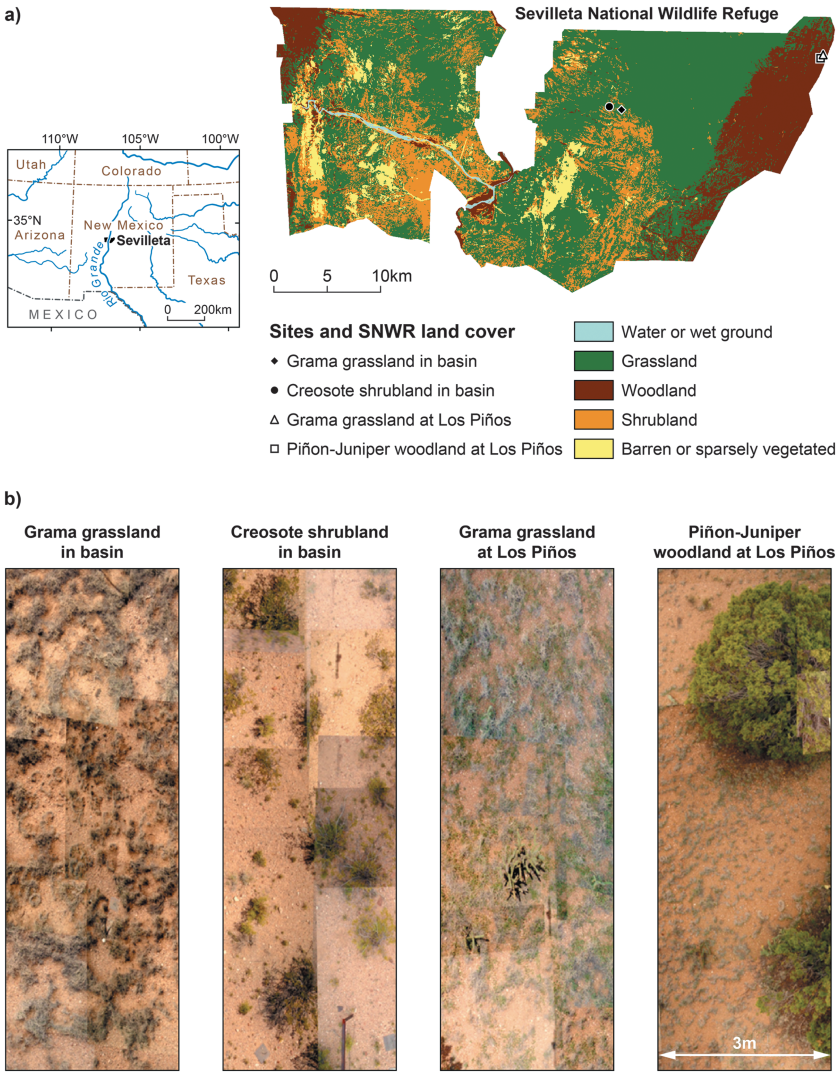


**Figure 1.** Location and vegetation coverage of study sites: (a) SNWR location in New Mexico and location of study sites within the SNWR and direction of woody encroachment into grasslands. Source data: 0.5 ha normalized difference vegetation index thematic mapper image 1987–1993 [*Sevilleta LTER*, 2014]. The arrows on the SNWR map indicate directions of woody encroachment into grassland. (b) Mosaicked close range aerial photos of subsection of each sampling site to illustrate variation in vegetation cover and pattern. Site locations: grama grassland in basin (34°20′23.67″N, 106° 43′44.04″W), creosote shrubland (34°20′16.78″N, 106°44′17.70″W), grama grassland at Los Piños (34°23′17.88″N, 106°31′27.89″W), and piñon-juniper woodland (34°23′12.42″N, 106°31′36.73″W).

basin and creosote shrubland) were located over the transition between Turney Loam and Nickel-Caliza very gravelly sandy loam series. At the bordering Los Piños mountain sites (grama grassland at Los Piños and piñon-juniper woodland), the study sites were located on the Puertecito series, which is also a gravelly sandy loam [*U.S. Department of Agriculture, Soil Survey*, 2014]. Soils across the study sites were relatively shallow and in the basin underlain by an impermeable calcium carbonate "caliche" layer between 15 and 45 cm below the soil surface. The SNWR experiences a semiarid climate, in which the main limiting resource is water. The long-term mean annual precipitation (1989–2002) is 250 mm in the lower elevation basin sites and 365 mm in the mountain sites [*Sevilleta LTER*, 2014]. Precipitation is influenced by the Pacific Decadal Oscillation and El Niño–Southern Oscillation climatic cycles. Precipitation at the SNWR is typically dominated by a summer monsoon season, with around 60% of annual precipitation falling in a small number of short-duration, high-intensity rainfall events between June and September. The long-term mean annual temperatures (1989–2002) are 13.2°C in the basin and 12.7°C in the Los Piños mountains [*Sevilleta LTER*, 2014].

At the SNWR (Figure 1), as with the observed encroachment across the southwestern U.S., evidence suggests that human settlement over the last 150 years caused the current episode of change, attributed primarily to grassland degradation by cattle grazing and fire suppression, between 1936 and 1973 [*U.S. Fish and Wildlife Service*, 2014], exacerbated by periods of drought [*Buffington and Herbel*, 1965; *Peters et al.*, 2006; *Van Auken*, 2009]. Aerial photos provide evidence for the enlargement of woody clusters into grasslands [*Gosz*, 1992], and biogeochemical studies suggest the previous presence of grasslands in areas now dominated by woody vegetation [*Turnbull et al.*, 2008b; *Puttock et al.*, 2012].

Sites were chosen to represent "pristine" grama grassland (*Bouteloua* sp.) and creosote shrubland (*Larrea tridentata*) encroaching across the Rio Grande basin and piñon-juniper woodland (*Pinus edulis-Juniperus monosperma*) encroaching downslope in the Los Piños mountains. These vegetation changes are characteristic of those occurring across large extents of the semiarid basin and range landscape of the southwestern U.S. [*Eldridge et al.*, 2011; *Van Auken*, 2009]. The criteria used in the selection of the sites were (a) each site must be characteristic of an end-member vegetation state over the two monitored ecotones; (b) sites must be of comparable area, dimensions, and slope to allow comparison between monitored rainfall-runoff relationships; (c) sites must be located on a planar interfluve slope; and (d) at the two ecotones, sites selected as being representative of end-member vegetation states must be as close as possible, thus minimizing variation in geology, soil characteristics, and meteorological variables.

## 3. Methods

### 3.1. Experimental Design

Selected study sites each encompassing an area of 300 $m^2$ (10 m wide and 30 m long) within an interfluve geomorphic position, with length being particularly important as 30 m, represented the typical hillslope length in these dissected landscapes and has been shown to have a significant influence on rainfall-runoff relationships and transmission losses [*Parsons et al.*, 2006]. The gradient of the selected sites was 4% at the grama grassland in basin site, 3% at the creosote shrubland site, 7% at the grama grassland at Los Piños site, and 6% at the piñon-juniper woodland site. Sites were sampled for eroded sediment, soil, and vegetation. Each study site consisted of a bounded and instrumented runoff plot, chosen for their ability to quantify fluxes of water, sediment, and nutrients [*Wainwright et al.*, 2000]. Rainfall-runoff event characteristics were monitored using a tipping-bucket rain gauge and an instrumented supercritical flume, both recording on a 1 min time interval. All eroded sediments from monitored runoff-generating events (between 8 and 11 per site collected during the 2010 and 2011 monsoon season) were collected for analysis [*Puttock et al.*, 2013; *Turnbull et al.*, 2010b]. Soil samples (0–5 cm depth) were collected at each site ($N = 90$) using a nested geostatistical sampling strategy, with the vegetation cover recorded for each sample [*Turnbull et al.*, 2010a]. In 2010, representative vegetation (leaf) samples ($N = 10$) were collected using a randomized quadrat sampling strategy [*Puttock et al.*, 2012]. The spatial coverage and pattern of vegetation cover at each site was classified using close range aerial photos [*Puttock et al.*, 2013]. Images were compiled using Erdas Imagine 2011 then imported into Esri Arc View (v 9.3.1), manually digitized, and classified into three classes: bare ground, woody vegetation cover, and grass vegetation cover. The calculated percentage vegetation and bare ground cover at each site were as follows: grama grassland in basin site = 55% grass and 45% bare; creosote in basin site = 21% woody and 79% bare; grama grassland at Los Piños site = 61% grass and 39% bare; and piñon-juniper at Los Piños = 9% grass, 29% woody, and 62% bare [*Puttock et al.*, 2013].

### 3.2. Sample Analysis

Soil and vegetation samples were prepared for analysis by oven drying at 60°C to a constant weight after which soil was sieved (<2 mm) and ground to a fine powder. Soil samples were washed in 2 M HCL to remove carbonates. Samples were analyzed for total organic C and bulk $\delta^{13}C$ using a Carlo Erba NA2000 analyzer (CE Instruments, Wigan, UK) interfaced to a SerCon 20–22 isotope ratio mass spectrometer (SerCon Ltd., Crewe, UK). Wheat flour ($N = 1.91\%$, $C = 41.81\%$, $^{15}N = 4.8‰$, and $^{13}C = -26.4‰$) calibrated against International Atomic Energy Agency N-1 by Iso-Analytical, Crewe, UK, was used as a reference standard [*Puttock et al.*, 2012]. The analytical precision of the $\delta^{13}C$ measurements was <0.1‰, and duplicates of all samples were run. The $\delta^{13}C$ values were expressed relative to Vienna Peedee belemnite:

$$^{13}C\ (‰) = \left[\left(\text{atom}\%\,^{13}C_{\text{sample}} - \text{atom}\%\,^{13}C_{\text{VPDB}}\right)/\text{atom}\%\,^{13}C_{\text{VPDB}}\right] \times 1000 \quad (1)$$

**Table 1.** Biogeochemical Signatures of Vegetation[a,b]

| Vegetation (*N*) | $\delta^{13}$C ‰ | % $C_{31}$ | $C_{27}$:$C_{31}$ |
|---|---|---|---|
| Grama grass (10) | −14.7 ± 0.2a | 35.1 ± 4.12a | 0.05 ± 0.01a |
| Creosote (10) | −25.9 ± 0.3b | 5.9 ± 1.48b | 9.87 ± 2.17b |
| Piñon (10) | −24.9 ± 0.3c | 21.3 ± 6.02c | 1.43 ± 0.40c |
| Juniper (10) | −24.0 ± 0.1c | 6.5 ± 0.93b | 0.01 ± 0.09d |

[a]For each study site, values followed by the same letter are not significantly different, while values followed by a different letter are significantly different ($p < 0.05$).
[b]Bulk $\delta^{13}$C values (‰), mean percentage contribution of $C_{31}$ *n*-alkane, and ratio of $C_{27}$:$C_{31}$ ($N$ = 10) of leaves randomly sampled in June 2010 from the dominant vegetation types in 300 $m^2$ sites representing the two predominant grass to shrub transitions at the SNWR. For all values, ± denotes standard error.

The proportion of organic C in soil and eroded sediment derived from $C_4$ grass sources was estimated from the vegetation input values using a mass balance equation [*Boutton et al.*, 1999]:

$$\%\ C_4 = ((\delta_s - \delta_3)/(\delta_4 - \delta_3)) \times 100 \quad (2)$$

where $\delta_s$ = sample $\delta^{13}$C (‰), $\delta_3$ = $C_3$ woody vegetation $\delta^{13}$C (‰), and $\delta_4$ = $C_4$ grass vegetation $\delta^{13}$C (‰).

To prepare samples for *n*-alkane analysis, total lipid extraction was undertaken, followed by lipid fractionation to extract the hydrocarbon fraction. The method was adopted from *Van Bergen et al.* [1998] and involved (i) soxhlet extraction of sample (1 g vegetation and 10 g soil) for 24 h using dichloromethane (DCM):acetone (v.v 9:1) high-performance liquid chromatography grade organic solvents plus the addition of 10 μL 1 μg/μL tetratriacontane (98% Acros Organics) internal standard (IS) solution, (ii) evaporation of solvent following extraction and resuspension in DCM:methanol (v.v 2:1), and (iii) fractionation of extracted lipids using flash column chromatography using silica gel (60 Å particle size) as the stationary phase and hexane as the eluent.

Analysis to determine *n*-alkane concentrations used an Agilent 7890A gas chromatograph with an Agilent 1909 J-413HP-5 phenylmethlysiloxane column (30 m × 320 μm × 0.25 μm). Initial oven temperature was 40°C with a 20°C/min increase to 130°C, followed by a 4°C/min increase to 300°C, then held at 300°C for 10 min. Due to the well-documented odd-over-even predominance of *n*-alkanes and even spacing on the chromatogram, long chain *n*-alkanes ($C_{27}$–$C_{35}$) were identified by elution order relative to the IS and confirmed using a National Institute of Standards and Technology library. The concentration of *n*-alkanes in samples was calculated relative to the IS of known concentration. Interpretation of *n*-alkane results used the percentage distribution of $C_{31}$ and the ratio between the shorter chain $C_{27}$ (indicative of woody source [*Zech et al.*, 2009]) and longer chain $C_{31}$ (indicative of grass source [*Eckmeier and Wiesenberg*, 2009]).

### 3.3. Statistical Analysis

To establish whether the observed variance between sites was significant, an independent two-tailed heteroscedastic *t* test was used. The test assumed unequal variance between samples. The strength of the relationships between discharge and event organic C losses at each site was tested via linear regression, while analysis of covariance (ANCOVA) was used to test for variance between the study sites once variation in discharge was accounted for. All statistical analyses were conducted using SPSS v16 (SPSS Inc., Chicago, IL, USA) at the 95% confidence level ($p < 0.05$).

## 4. Results

### 4.1. Biogeochemical Signatures of Vegetation Species

Analysis of key input vegetation species showed that grama grass had a different biogeochemical signature to that of the three woody species in the basin or montane sites (Table 1). As piñon and juniper in the SNWR and southwestern U.S. commonly grow in mixed stands, [*Wilcox et al.*, 2003a] and as the landscape scale form a common woody end-member community, an amalgamated piñon-juniper bulk $\delta^{13}$C value was also calculated. The bulk $\delta^{13}$C values of grama grass ($\delta^{13}$C = −14.7‰ ± 0.2) were enriched relative to woody species (creosote: $\delta^{13}$C = −25.9‰ ± 0.3; piñon-juniper: $\delta^{13}$C = −24.5‰ ± 0.8). The *n*-alkane signature of grama grass was dominated by $C_{31}$ and $C_{33}$ *n*-alkanes, while that of creosote and piñon woody species had a greater relative abundance of the shorter chain $C_{27}$ homologue, with consequently increased $C_{27}$:$C_{31}$ ratios.

**Table 2.** Site Soil Characteristics[a]

| Study Site | Cover[b] (*n*) | >2 mm Particle (%) | Mean SOC ± SE (mg cm$^{-3}$) | Mean Weighted SOC ± SE (mg cm$^{-3}$) |
|---|---|---|---|---|
| Grama grassland in basin | B (44) | 25.3 ± 1.33a | 2.69 ± 0.06a | 3.08 ± 0.06a |
| | G (46) | 15.2 ± 1.70b | 3.40 ± 0.07a | |
| Creosote in basin | B (47) | 32.7 ± 0.96c | 2.42 ± 0.15a | 3.10 ± 0.13a |
| | C (43) | 13.4 ± 1.38b | 5.69 ± 0.13b | |
| Grama grassland at Los Piños | B (42) | 38.9 ± 0.81d | 12.13 ± 0.34a | 12.26 ± 0.16b |
| | G (48) | 38.8 ± 1.26d | 12.34 ± 0.26a | |
| Piñon-juniper at Los Piños | B/G (40) | 40.6 ± 1.02d | 13.53 ± 0.09a | 15.48 ± 0.30c |
| | PJ (50) | 27.7 ± 1.28a | 21.42 ± 0.24b | |

[a]Descriptive analysis of vegetation cover, particle size (>2 mm %), and mean soil organic carbon content (mg cm$^{-3}$) across the study sites, separated by cover and a compiled site value weighted by percentage vegetation cover. For all values, ± denotes standard error.
[b]Cover: B = bare, G = grass, C = creosote, and PJ = piñon-juniper. For each study site, values followed by the same letter are not significantly different, while values followed by a different letter are significantly different ($p < 0.05$).

Juniper had a notably different *n*-alkane signature to the other woody species, showing no significant difference ($p > 0.05$) in $C_{27}$:$C_{31}$ with that of grass. However, as piñon and juniper both had a significantly enriched $\delta^{13}C$ value ($p < 0.05$) and the application of the two biogeochemical analyses in combination permitted increased understanding of the sources of organic C in both soils and fluvially eroded sediments.

### 4.2. Change in SOC

Areally weighted values (Table 2) indicated that there were significant differences in the spatial distribution of SOC in the surface soil between grassland (grama grassland in basin and grama grassland at Los Piños) and woody sites (creosote shrubland and piñon-juniper woodland). The mountain soils at Los Piños contained more SOC ($p < 0.05$) than the basin soils regardless of vegetation cover, underlining the importance of understanding site-specific variations. However, over both ecotones, the mean bulk $\delta^{13}C$ values of soil were elevated at the grama grassland sites relative to the woody sites ($p < 0.05$), indicating the dominance of $C_4$ grass-derived C (Table 3). There was no difference ($p > 0.05$) in soil bulk $\delta^{13}C$ values under bare or vegetated areas in the grassland sites, which contrasted with the woody sites where the soil from bare areas had enriched $\delta^{13}C$ values, and therefore a greater proportion of grass-derived C, compared to vegetated areas. The *n*-alkane profiles of soils in the grama grassland sites in both the basin and Los Piños mountain sites were dominated by $C_{31}$ (approximately 60%), and there was no significant difference between bare versus vegetated areas ($p > 0.05$). At the creosote shrubland site, $C_{27}$ concentrations were greater ($p < 0.05$) in soils beneath creosote bushes (27%) than from bare soils (10%), while $C_{31}$ concentrations were less ($p < 0.05$) in soils beneath creosote bushes (10%) than from bare soils (19%), confirming a predominance of grass C in bare soil areas at woody sites. As a result of greater $C_{27}$ concentrations from woody C input, soils

**Table 3.** Biogeochemical Signatures of Surface Soil[a]

| Study Site | Cover[b] (*N*) | Mean $\delta^{13}C$ ‰ | Site Mean $\delta^{13}C$ ‰ | Site Mean % $C_4$ | % $C_{31}$ | $C_{27}$:$C_{31}$ |
|---|---|---|---|---|---|---|
| Grama grassland in basin | B(44) | −18.58 ± 0.20a | −19.9 ± 0.2a | 55.52 ± 2.3a | 64.8 ± 22.05a | 0.1 ± 0.11a |
| | G(46) | −19.09 ± 0.18a | | | 66.3 ± 21.38a | 0.06 ± 0.03a |
| Creosote shrubland | B (47) | −21.51 ± 0.19a | −22.1 ± 0.4b | 23.62 ± 3.8b | 18.7 ± 5.04b | 0.54 ± 0.14b |
| | C (43) | −22.76 ± 0.18b | | | 10.9 ± 2.87c | 1.81 ± 0.25c |
| Grama grassland at Los Piños | B (42) | −18.21 ± 0.19a | −18.9 ± 0.2a | 56.85 ± 5.4a | 67.7 ± 17.34a | 0.12 ± 0.03a |
| | G (48) | −18.43 ± 0.17a | | | 64.4 ± 21.41a | 0.09 ± 0.03a |
| Piñon-juniper woodland | B/G (40) | −19.33 ± 0.32a | −20.3 ± 0.4c | 42.17 ± 4.1c | 3.6 ± 1.16d | 0.58 ± 0.20b |
| | PJ(50) | −21.96 ± 0.42b | | | 3.4 ± 1.17d | 1.31 ± 0.32c |

[a]Mean bulk $\delta^{13}C$ values (‰). (*N* in brackets following cover type), mean percentage contribution of $C_{31}$ *n*-alkanes, and ratio of $C_{27}$:$C_{31}$. (*N* = 10). For all values, ± denotes standard error.
[b]Cover: B = bare, G = grass, C = creosote, and PJ = piñon-juniper. For each study site, values followed by the same letter are not significantly different, while values followed by a different letter are significantly different ($p < 0.05$).

**Table 4.** Hydrological Response to Rainfall Events Over Study Sites[ab]

| Site (*N*) | RC | *Q* (l m$^{-2}$) | ES (g m$^{-2}$) | >2 mm (%) | OC (g m$^{-2}$) |
|---|---|---|---|---|---|
| Grama grassland in basin (9) | 0.04 ± 0.02a | 0.32 ± 0.19a | 0.77 ± 0.35a | 4.2 ± 0.8a | 0.003 ± 0.00a |
| Creosote shrubland (10) | 0.11 ± 0.03b | 1.31 ± 0.65b | 3.44 ± 1.37b | 9.6 ± 0.9b | 0.112 ± 0.09b |
| Grama grassland at Los Piños (11) | 0.07 ± 0.02a | 0.50 ± 0.19a | 1.22 ± 0.61c | 4.1 ± 0.7a | 0.030 ± 0.02c |
| Piñon-juniper woodland (8) | 0.12 ± 0.03b | 1.41 ± 0.41b | 4.54 ± 1.52b | 8.1 ± 1.0b | 0.151 ± 0.051b |

[a]For each study site, values followed by the same letter are not significantly different, while values followed by a different letter are significantly different ($p < 0.05$).
[b]RC = runoff coefficient; *Q* = total mean discharge; ES = eroded sediment yield, >2 mm % = particle size greater than 2 mm; and OC = mean organic carbon yields, normalized per unit area. Results include standard error values, while results followed by the same letter are not statistically significant ($p < 0.05$). The numbers in brackets following study site name denote number of rainfall-runoff events from which mean values are derived. For all values, ± denotes standard error.

from both woody-dominated sites had higher $C_{27}$:$C_{31}$ ratios and greater heterogeneity between woody and bare/grass areas, where ratio values were higher ($p < 0.05$) under woody cover. In summary, the combined bulk $\delta^{13}C$ and *n*-alkane profiles of soils demonstrated that the grassland was the legacy ecotype in both locations and that grasslands had been encroached by woody vegetation (creosote in the basin or piñon-juniper at Los Piños).

### 4.3. Change in Eroded Sediment and Organic C

Across both monitored grass-woody ecotones, woody sites showed an accentuated hydrological response to rainfall (Table 4) exhibiting significantly greater rainfall-runoff coefficients ($p < 0.05$). Precipitation in these dryland environments is highly variable both spatially and temporally, yet there was no significant difference in rainfall received between the woody sites and their comparative grassland site ($p > 0.05$); woody sites also showed significantly greater event discharge ($p < 0.05$). The erosion and loss of sediment-associated organic C by water varied with rainfall-runoff event characteristics, with all sites showing significant positive linear relationships ($p < 0.05$) between event discharge and organic C losses (Figure 2; $R^2$ values for each site: grama grassland in basin = 0.98, creosote shrubland = 0.89, grama grassland at Los Piños = 0.85, and piñon-juniper = 0.67). However, ANCOVA analysis, using discharge as the covariate, showed there to be a significant variance in organic C losses between sites ($p < 0.05$, model fit $R^2 = 0.79$). Regression relationships showed steeper trendlines and higher maxima for the woody sites indicating an accentuated hydrological response relative to grassland sites (Figure 2). Additionally, eroded sediment at all sites showed a reduction in particle size (Table 4) as shown by the percentage contribution of the >2 mm fraction relative to surface samples (Table 2), indicating that preferential entrainment and transport of fine material were occurring. Additionally, a higher

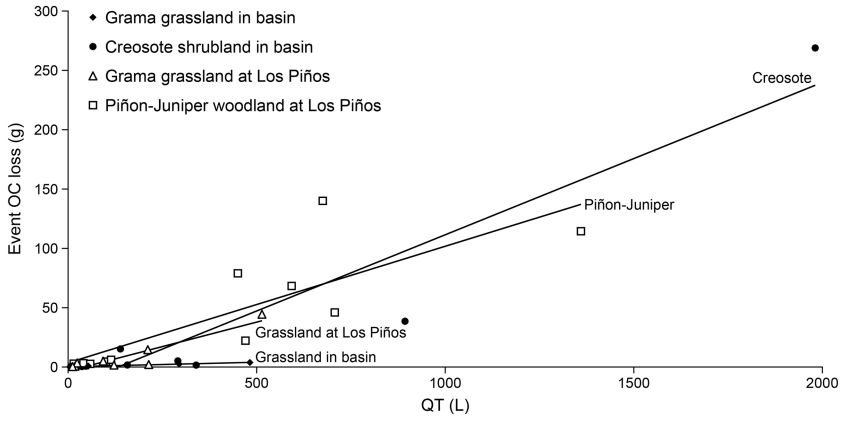


**Figure 2.** Relationship between runoff and C erosion: relationship between total event discharge (QT L) and eroded organic carbon yield (OC loss g) from each site. The solid lines represent best linear fits to data from each site to illustrate the overall trend of hydrological response resulting in erosion of organic carbon but at decreasing rates in grass compared to woody-dominated landscapes. $R^2$ values for each site: grama grassland in basin = 0.98, creosote shrubland = 0.89, grama grassland at Los Piños = 0.85, and piñon-juniper = 0.67. At each site, the linear relationships between QT and OC loss are statistically significant ($p < 0.05$).

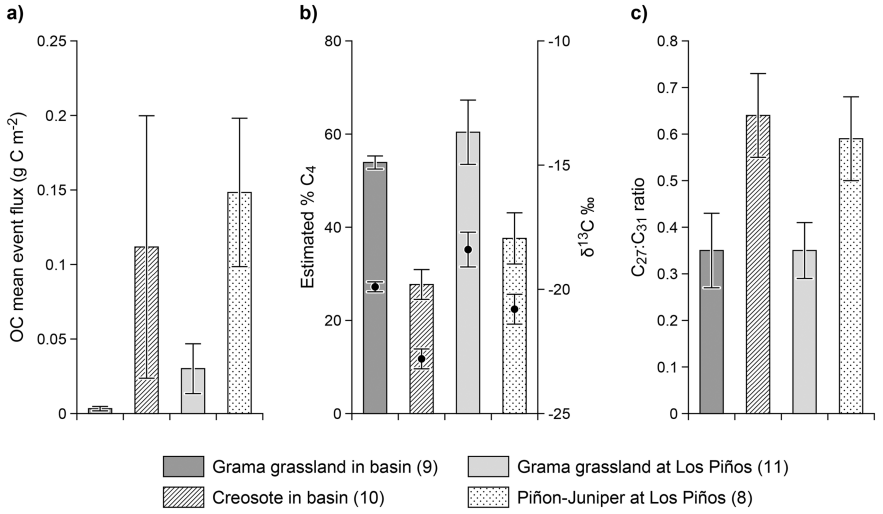


**Figure 3.** Summary result graphs. (a) Magnitude of event organic carbon fluxes (g C $m^{-2}$). (b) Estimated percentage of $C_4$ organic carbon in eroded sediment and bulk $\delta^{13}C$ values from which these are calculated (‰). (c) Ratio of $C_{27}$:$C_{31}$ *n*-alkane homologue concentration in eroded sediment. The numbers in brackets (*N*) following study site name denote number of rainfall-runoff events from which mean values are derived. The error bars denote standard error for presented mean values.

percentage of >2 mm material was lost from the woody sites, which in addition to higher total discharge event and sediment yields illustrates the greater erosive potential of woody sites. Consequently, event organic C losses via erosion (Figure 3) were significantly greater ($p < 0.05$) from woody sites than from grassland sites (grama grassland in basin: $0.003 \pm 0.00$ g $m^{-2}$, grama grassland at Los Piños: $0.030 \pm 0.02$ g $m^{-2}$, creosote shrubland: $0.112 \pm 0.09$ g $m^{-2}$, and piñon-juniper woodland $0.151 \pm 0.051$ g $m^{-2}$).

Despite site- and species-specific differences in SOC characteristics, event flux data revealed only minor differences between creosote shrubland and piñon-juniper sites or between the two grama grassland sites (Table 4). Once woody encroachment had occurred, regardless of the woody species involved, the two ecotones responded in a similar manner in terms of water, sediment, and organic C losses. Sediment eroded from the grama grassland sites had greater bulk $\delta^{13}C$ values ($-19.9‰ \pm 0.2$ in basin and $-18.4‰ \pm 0.7$ at Los Piños) and lower $C_{27}$:$C_{31}$ ratios ($0.35 \pm 0.08$ in basin and $0.35 \pm 0.06$ grama at Los Piños; Table 5) relative to the creosote shrubland (bulk $\delta^{13}C = -22.8 \pm 0.4$ and $C_{27}$:$C_{31} = 0.64 \pm 0.09$) and piñon-juniper woodland sites (bulk $\delta^{13}C = -20.8‰ \pm 0.6$ and $C_{27}$:$C_{31} = 0.59 \pm 0.09$). $C_{27}$:$C_{31}$ ratios in sediments eroded from the creosote shrubland site were significantly lower ($p < 0.05$) than those in either creosote vegetation samples or surface soil samples taken from under creosote vegetation. In contrast, there was no significant difference ($p > 0.05$) between the $C_{27}$:$C_{31}$ and $C_{29}$:$C_{31}$ ratios in bare soil and eroded sediment. Thus, grass-sourced organic C dominated erosive losses from the grama grassland sites but also constituted a significant proportion of organic C eroded from woody sites comprising 28% at the creosote shrubland site and 38% at the piñon-juniper woodland site as indicated by $\delta^{13}C$ values (Table 5) and accompanied by a reduction in $C_{27}$:$C_{31}$ ratios ($p < 0.05$). The bulk $\delta^{13}C$ values and *n*-alkane signatures of the eroded soils from the piñon-juniper woodland and creosote

**Table 5.** Biogeochemical Signatures of Eroded Sediment[a, b]

| Site (*N*) | $\delta^{13}C$ ‰ | % $C_4$ | % $C_{31}$ | $C_{27}$:$C_{31}$ |
|---|---|---|---|---|
| Grama grassland in basin (9) | $-19.9 \pm 0.2^a$ | $53.9 \pm 1.4^a$ | $41.23 \pm 2.25^a$ | $0.35 \pm 0.08^a$ |
| Creosote shrubland (10) | $-22.8 \pm 0.4^b$ | $27.7 \pm 3.2^b$ | $35.80 \pm 3.35^b$ | $0.64 \pm 0.09^b$ |
| Grama grassland at Los Piños (11) | $-18.4 \pm 0.7^a$ | $60.4 \pm 6.9^c$ | $25.25 \pm 1.59^c$ | $0.35 \pm 0.06^a$ |
| Piñon-Juniper woodland (8) | $-20.8 \pm 0.6^c$ | $37.6 \pm 5.5^d$ | $20.37 \pm 1.09^d$ | $0.59 \pm 0.09^b$ |

[a]For each study site, values followed by the same letter are not significantly different, while values followed by a different letter are significantly different ($p < 0.05$).
[b]Mean bulk $\delta^{13}C$ values (‰) ± SE, mean percentage contribution of $C_{31}$, and ratio of $C_{27}$:$C_{31}$. The numbers in brackets following study site name denote number of rainfall-runoff events from which mean values are derived. For all values, ± denotes standard error.

shrubland sites demonstrated the enhanced loss of legacy grassland (and therefore previously stable) SOC from sites undergoing woody encroachment.

## 5. Discussion

### 5.1. Change in Soil C Dynamics Over Vegetation Transitions

Focusing on two widely occurring dryland ecotones, our research showed that the transition from grassland to woody vegetation was accompanied by significant changes in the amount and spatial distribution of SOC. Furthermore, results showed that woody-dominated sites exhibited an accentuated hydrological response to rainfall leading to greater event organic C losses. Results agree with previous research in dryland environments that have found rainfall-runoff coefficients [*Schlesinger et al.*, 2000], event discharge, and erosion rates to be notably higher from woody compared to grassland environments [*Parsons et al.*, 1996; *Wainwright et al.*, 2000]. Previous monitoring [*Turnbull et al.*, 2010a] over the grass-creosote shrubland ecotone in the basin at the SNWR found higher runoff coefficients on the creosote shrubland site (0.28) compared to the grama grassland site (0.15 for events monitored) and C losses by fluvial erosion to be 6 times higher from creosote-dominated sites [*Brazier et al.*, 2013]. This study builds upon previous work at the SNWR, demonstrating that despite species and site-specific differences, the grass-piñon-juniper ecotone shows a comparable directional change in hydrological response and associated sediment and C losses. In a study into nutrient losses via fluvial erosion in a comparable dryland environment, *Barger et al.* [2006] highlighted the importance of particulate bound organic C fluxes concluding that >98% of the total C losses were from sediment sources, being highly correlated with the total sediment loss. Therefore, the observed organic C losses raises important questions over the stability of this important C store in such environments.

Overall, as has previously been found [*Jackson et al.*, 2002], the woody-dominated sites had slightly higher areally weighted SOC levels, but more notably a redistribution in spatial distribution [*Throop and Archer*, 2008], with greater spatial heterogeneity with higher SOC concentrations under vegetation, compared with comparative bare (or degraded grass) soils (Table 2). Thus, results support previous research finding that woody encroachment in drylands can result in a major change in ecosystem structure [*Bai et al.*, 2009; *Bird et al.*, 2002; *Havstad et al.*, 2006; *Schlesinger et al.*, 1990], characterized by an increased heterogeneity of vegetation and SOC distribution [*Puttock et al.*, 2013]. Reduction in vegetation cover following woody encroachment decreases vegetative protection of the soil [*Ludwig et al.*, 2005] and increases connectivity [*Mayor et al.*, 2008; *Wainwright et al.*, 2011], leading to accentuated water erosion fluxes [*Parsons et al.*, 1996; *Wilcox et al.*, 2003a]. Greater variation in SOC contents at the woody sites (Table 2) supports the theory that the alteration of hydrological functions associated with woody encroachment results in the occurrence of positive feedback mechanisms [*Peters and Herrick*, 2001] reinforcing the heterogeneous woody landscape structure into islands of fertility [*Schlesinger et al.*, 1990]. The underlying mechanism is illustrated by event organic C yields showing that woody encroachment results in increased event losses of organic C via fluvial erosion [*Barger et al.*, 2011; *Brazier et al.*, 2013]. These changes may be irreversible and become more widespread unless such dryland landscapes are actively managed to prevent woody species encroachment into grasslands.

In addition to erosion by water addressed in this study, there is a need for further understanding of the role of wind erosion upon C dynamics in these landscapes. The aeolian redistribution of fine, easily erodible material is thought to be the other key geomorphic agent acting in these dryland environments [*Ravi et al.*, 2010; *Okin et al.*, 2009]. The increased percentage of bare ground at woody sites reported in this study may result in a greater susceptibility to wind erosion [*Gillette and Monger*, 2006]. However, no data exist to quantify the aeolian flux of C or compare directly with the fluvial fluxes presented herein.

As discussed, soil C and erosion are an area of the C budget over which there is major uncertainty [*Lal*, 2005], and results presented show that fluvial erosion increases significantly following woody encroachment. Nonetheless, it is only one component of the ecosystem C cycle. Woody encroachment into drylands will also alter biomass [*Fang et al.*, 2001; *Asner et al.*, 2003] with an increase in aboveground biomass being reported for piñon-juniper woodland [*Turner et al.*, 2005] but a decrease reported for creosote shrubland [*Cross and Schlesinger*, 1999]. Primary productivity may also change, with implications for the dynamic replacement or depletion of SOC in landscapes undergoing erosion [*Berhe et al.*, 2007; *Nadeu et al.*, 2012]. Previous research has shown no significant change in annual net primary following creosote shrub encroachment but an

increase in piñon-juniper woodland [*Turner et al.*, 2005; *Muldavin et al.*, 2008]. Gaseous $CO_2$ fluxes show a large degree of interannual variability, being highly responsive to meteorological variables [*Mielnick et al.*, 2005] but with *Emmerich* [2003] also showing a higher $CO_2$ flux from woody-dominated sites. Therefore, other components of the C cycle will also influence whether woody encroachment and concurrent change in ecosystem function result in a net source or sink of C.

### 5.2. Change in the Source of C Over Vegetation Transitions

Dual-proxy biogeochemical analysis illustrated that the spatial heterogeneity of SOC sources increased following woody encroachment. In grassland sites, the homogeneity of *n*-alkanes distribution was evident in the bare and vegetated soils which displayed no significant difference for natural abundant stable $\delta^{13}C$ isotope signature and *n*-alkane profiles ($p > 0.05$). In contrast, the creosote shrubland site displayed a much greater degree of heterogeneity in *n*-alkane distributions most clearly represented by $C_{27}$:$C_{31}$ ratio of the soil samples. In soil collected from under creosote vegetation, the ratio values were significantly higher ($p < 0.05$), illustrating a much greater input of woody vegetation, as would be expected from the current creosote vegetation cover. However, soils in bare areas showed a significantly greater amount of $C_{31}$ and significantly lower ratio values ($p < 0.05$). This result was of high importance, supporting the largely anecdotal evidence that shrub dominated the areas across the basin study area that is used to be dominated by grasses [*Buffington and Herbel*, 1965]. At the Los Piños sites, due to the similarities between grama grass and juniper *n*-alkane signatures, there was a degree of difficulty in determining between sources; based upon *n*-alkane signature, a problem was previously experienced when using *n*-alkane signatures alone [*Marschner et al.*, 2008; *Gocke et al.*, 2011]. However, the use of *n*-alkane signatures from piñon and combined with the $\delta^{13}C$ values of both piñon and juniper demonstrated that the same trends transcend to the mountainous, grassland to piñon-juniper transition [*Wilcox et al.*, 2003b]. Evidence of legacy grass-C in bare areas has been observed in other southwestern U.S. landscapes following woody encroachment [*Boutton et al.*, 1999; *Bai et al.*, 2012 ]. Results over both transitions provide quantitative evidence supporting the theory that, following woody encroachment in these dryland environments, new organic material is primarily concentrated in resource "islands" under vegetation patches [*Schlesinger et al.*, 1990].

The magnitude of event C losses was increased by accelerated fluvial erosion following woody encroachment, with biogeochemical analysis indicating that the sources of the eroded organic C were also more variable, with both *n*-alkane and stable $\delta^{13}C$ isotopes demonstrating a notable grass-sourced contribution to eroded SOC. Results demonstrating the linkages between soil in bare interpatch areas and eroded sediment were noteworthy, signifying that most of the soil eroded from the creosote site during rainfall-runoff events originates from the bare interpatch areas. Bare areas are more susceptible to erosion [*Reid et al.*, 1999; *Ridolfi et al.*, 2008; *Wainwright et al.*, 2011], and thus, following the increase in bare ground following woody encroachment, these areas have the potential to become a significant source of organic C event losses from a previously stabilised (or buried) pool.

There is a requirement to extend the findings presented within this study to the landscape and catchment scales thus, addressing to what extent the eroded organic C is locally redistributed within the landscape or reaches connected river networks resulting in ecosystem loss [*Okin et al.*, 2009]. The combined use of stable $\delta^{13}C$ isotope signature and *n*-alkane signatures has been shown in this study to provide a technique to understand the source of *s* = organic C. Therefore, supported by previous research that has used these techniques to understand the source of sediment in rivers [*Wu et al.*, 2007], it is suggested that the biogeochemical tracing techniques used herein can be used for the investigation of the source and fate of eroded sediment and organic C at the landscape or catchment scale.

## 6. Conclusion

In this study we observed that woody encroachment in dryland ecosystems can create a heterogeneous vegetation structure and coincident variability in SOC resources. Combined with changes in hydrological function, changes in ecosystem structure may precipitate a potentially catastrophic shift to a much less stable ecosystem state [*Turnbull et al.*, 2008a] with an increased vulnerability to fluvial erosion. Data from two woody landscapes in basin and montane ecotones, which may be analogous with large areas of the basin and range southwestern U.S., showed that not only more organic C was eroded per unit area than in pristine grasslands

but that this included large quantities of previously stabilized organic C from legacy grasslands. While there remains a disagreement over the role of soil erosion in the C budget [*Berhe et al.*, 2007; *Lal*, 2003], it is acknowledged that erosion alters soil-atmosphere C fluxes [*Van Oost et al.*, 2007] and can enhance soil-atmosphere C fluxes in drylands [*Emmerich*, 2003]. There is a need for further landscape scale research, encompassing all components of the carbon budget in these dryland environments, and we suggest that the transition from grassland to woody environments should be actively managed to minimize losses by fluvial erosion.

**Acknowledgments**

This research was supported by the University of Exeter and Rothamsted Research North Wyke, NSF award DEB-0217774 to the University of New Mexico for the long-term Ecological Research, and a British Society for Geomorphology student travel grant. This work represents part of the BBSRC-funded programs at Rothamsted Research on Sustainable Soil Function and Bioenergy and Climate Change. Additional thanks go to Liz Dixon for IRMS analysis, Helen Jones for redrawing the figures, the Sevilleta LTER, and the Sevilleta USFWS for allowing access to field sites in the SNWR. Finally, we would like to thank the two anonymous reviewers and an Associate Editor for their constructive feedback which improved this paper. In line with the AGU publications data policy, all relevant data can be accessed by contacting the corresponding author.

## References

Archer, N. A. L., J. N. Quinton, and T. M. Hess (2011), Patch vegetation and water redistribution above and below ground in south-east Spain, *Ecohydrology*, *5*(1), 108–120, doi:10.1002/eco.210.

Archer, S. (1995), Tree-grass dynamics in a prosopis-thornscrub savanna parkland - reconstructing the past and predicting the future, *Ecoscience*, *2*(1), 83–99, doi:10.1097/00010694-197011000-00006.

Asner, G. P., S. Archer, R. F. Hughes, R. J. Ansley, and C. A. Wessman (2003), Net changes in regional woody vegetation cover and carbon storage in Texas Drylands 1937–1999, *Global Change Biol.*, *9*, 316–335, doi:10.1046/j.1365-2486.2003.00594.x.

Bai, E., T. W. Boutton, X. Ben Wu, F. Liu, and S. R. Archer (2009), Landscape-scale vegetation dynamics inferred from spatial patterns of soil delta C-13 in a subtropical savanna parkland, *J. Geophys. Res.*, *114*, G01019, doi:10.1029/2008JG000839.

Bai, E., T. W. Boutton, F. Liu, W. X. Wu, and S. Archer (2012), Spatial patterns of soil d13C reveal grassland-to-woodland successional processes, *Org. Geochem.*, *42*, 1512–1518, doi:10.1016/j.orggeochem.2010.11.004.

Barger, N. N., J. Herrick, J. Zee, and J. Belnap (2006), Impacts of biological soil crust disturbance and composition on C and N loss from water erosion, *Biogeochemistry*, *77*(2), 247–263, doi:10.1007/s10533-005-1424-7.

Barger, N. N., S. R. Archer, J. L. Campbell, C. Huang, J. A. Morton, and A. K. Knapp (2011), Woody plant proliferation in North American drylands: A synthesis of impacts on ecosystem carbon balance, *J. Geophys. Res.*, *116*, G00K07, doi:10.1029/2010JG001506.

Berhe, A. A., and M. Kleber (2013), Erosion, deposition, and the persistence of soil organic matter: Mechanistic considerations and problems with terminology, *Earth Surf. Processes Landforms*, *38*(8), 908–912, doi:10.1002/esp.3408.

Berhe, A. A., J. Harte, J. W. Harden, and M. S. Torn (2007), The significance of the erosion-induced terrestrial carbon sink, *BioScience*, *57*(4), 337–346, doi:10.1641/b570408.

Bhark, E. W., and E. E. Small (2003), Association between plant canopies and the spatial patterns of infiltration in shrubland and grassland of the Chihuahuan Desert, New Mexico, *Ecosystems*, *6*(2), 185–196, doi:10.1007/s10021-002-0210-9.

Bird, S. B., J. E. Herrick, M. M. Wander, and S. F. Wright (2002), Spatial heterogeneity of aggregate stability and soil carbon in semiarid rangeland, *Environ. Pollut.*, *116*, 445–455, doi:10.1016/S0269-7491(01)00222-6.

Boutton, T. W., S. R. Archer, and A. J. Midwood (1999), Stable isotopes in ecosystem science: Structure, function and dynamics of a subtropical Savanna, *Rapid Commun. Mass Spectrom.*, *13*(13), 1263–1277, doi:10.1002/(SICI)1097-0231(19990715)13:13<1263::AID-RCM653>3.0.CO;2-J.

Brazier, R. E., L. Turnbull, R. Bol, and J. Wainright (2013), Carbon loss by water erosion in drylands: Implications from a study of vegetation change in the southwest USA, *Hydrol. Processes*, *28*(4), 2212–2222, doi:10.1002/hyp.9741.

Breshears, D. D., M. H. Ebinger, and P. J. Unkefer (1999), Assessing carbon dynamics in semiarid ecosystems: Balancing potential gains with potential large rapid losses, *Natl. Res. Counc.*, *34*, 34–40.

Buffington, L. C., and C. H. Herbel (1965), Vegetational changes on a semidesert grassland range from 1858 to 1963, *Ecol. Monogr.*, *35*(2), 140–164, doi:10.2307/1948415.

Campbell, A., L. Miles, I. Lysenko, A. Hughes, and H. Gibbs (2008), Carbon storage in protected areas: Technical report, UNEP World Conserv. Monit. Cent., Cambridge, U. K.

Cross, A., and W. Schlesinger (1999), Plant regulation of soil nutrient distribution in the northern Chihuahuan Desert, *Plant Ecol.*, *145*(1), 11–25, doi:10.1023/a:1009865020145.

Dickie, J. A., and A. J. Parsons (2012), Eco-geomorphological processes within grasslands, shrublands and badlands in the semi-arid Karoo, South Africa, *Land Degrad. Dev.*, *23*(6), 534–547, doi:10.1002/ldr.2170.

Divine, C., and J. McDonnell (2005), The future of applied tracers in hydrogeology, *Hydrogeol. J.*, *13*(1), 255–258, doi:10.1007/s10040-004-0416-3.

D'Odorico, P., A. Bhattachan, K. F. Davis, S. Ravi, and C. W. Runyan (2013), Global desertification: Drivers and feedbacks, *Adv. Water Resour.*, *51*, 326–344, doi:10.1016/j.advwatres.2012.01.013.

Eckmeier, E., and G. L. B. Wiesenberg (2009), Short-chain n-alkanes (C16-20) in ancient soil are useful molecular markers for prehistoric biomass burning, *J. Archaeol. Sci.*, *36*(7), 1590–1596, doi:10.1016/j.jas.2009.03.021.

Eglinton, G., R. J. Hamilton, R. A. Raphael, and A. G. Gonzalez (1962), Hydrocarbon constituents of the wax coatings of plant leaves: A taxonomic survey, *Nature*, *193*(4817), 739–742, doi:10.1038/193739a0.

Eldridge, D. J., M. A. Bowker, F. T. Maestre, E. Roger, J. F. Reynolds, and W. G. Whitford (2011), Impacts of shrub encroachment on ecosystem structure and functioning: Towards a global synthesis, *Ecol. Lett.*, *14*, 709–722, doi:10.1111/j.1461-0248.2011.01630.x.

Emmerich, W. E. (2003), Carbon dioxide fluxes in a semiarid environment with high carbonate soils, *Agric. For. Meteorol.*, *116*(1), 91–102, doi:10.1016/S0168-1923(02)00231-9.

Eswaran, H., P. Reich, F. H. Beinroth, E. Padamnabhan, P. Moncharoen, and J. M. Kimble (2000), Global carbon stocks, in *Global Climate Change and Pedogeniccarbonates*, edited by R. Lal et al., pp. 15–25, Lewis Publishers, Boca Raton, Fla.

Fang, J., A. Chen, C. Peng, S. Zhao, and L. Chi (2001), Changes in forest biomass carbon storage in China between 1949 and 1998, *Science*, *292*, 2320–2322, doi:10.1126/science.1058629.

Gillette, D., and C. H. Monger (2006), Eolian processes on the Jornada Basin, in *Structure and Function of a Chihuan Desert Ecosystem*, edited by K. M. Havstad, L. F. Huenneke, and W. H. Schlesinger, pp. 189–211, Oxford Univ. Press, New York.

Gocke, M., Y. Kuzyakov, and G. L. B. Wiesenberg (2011), Differentiation of plant derived organic matter in soil, loess and rhizoliths based on n-alkane molecular proxies, *Biogeochemistry*, *112*, 23–40, doi:10.1007/s10533-011-9659-y.

Gosz, J. (1992), Ecological functions in a biome transition zone: Translating local responses to broad-scale dynamics, in *Landscape Boundaries SE - 3*, vol. 92, edited by A. Hansen and F. di Castri, pp. 55–75, Springer, New York, doi:10.1007/978-1-4612-2804-2_3.

Havstad, K. M., L. F. Huenneke, and W. H. Schlesinger (2006), *Structure and Function of a Chihuahuan Desert Ecosystem*, edited by LTER, Oxford Univ. Press, New York.
Higgins, S. I., and S. Scheiter (2012), Atmospheric $CO_2$ forces abrupt vegetation shifts locally, but not globally, *Nature*, *488*(7410), 209–212, doi:10.1038/nature11238.
Hurtt, G. C., S. W. Pacala, P. R. Moorcroft, J. Caspersen, E. Shevliakova, R. A. Houghton, and B. Moore (2002), Projecting the future of the U.S. carbon sink, *Proc. Natl. Acad. Sci. U.S.A.*, *99*(3), 1389–1394, doi:10.1073/pnas.012249999.
Jackson, R. B., J. L. Banner, E. G. Jobbagy, W. T. Pockman, and D. H. Wall (2002), Ecosystem carbon loss with woody plant invasion of grasslands, *Nature*, *418*, 623–626, doi:10.1038/nature00910.
Jansen, B., K. G. J. Nierop, J. A. Hageman, A. M. Cleef, and J. M. Verstraten (2006), The straight-chain lipid biomarker composition of plant species responsible for the dominant biomass production along two altitudinal transects in the Ecuadorian Andes, *Org. Geochem.*, *37*(11), 1514–1536, doi:10.1016/j.orggeochem.2006.06.018.
Jobbagy, E. G., and R. B. Jackson (2000), The vertical distribution of soil organic carbon and its relation to climate and vegetation, *Ecol. Appl.*, *10*(2), 423–436, doi:10.1890/1051-0761(2000)010[0423:TVDOSO]2.0.CO;2.
King, E. G., T. E. Franz, and K. K. Caylor (2012), Ecohydrological interactions in a degraded two-phase mosaic dryland: Implications for regime shifts, resilience, and restoration, *Ecohydrology*, *5*(6), 733–745, doi:10.1002/eco.260.
Knapp, A. K., et al. (2008), Shrub encroachment in North American grasslands: Shifts in growth form dominance rapidly alters control of ecosystem carbon inputs, *Global Change Biol.*, *14*, 615–623, doi:10.1111/j.1365-2486.2007.01512.x.
Lal, R. (2003), Carbon sequestration in dryland ecosystems, *Environ. Manage.*, *33*(4), 528–544, doi:10.1007/s00267-003-9110-9.
Lal, R. (2005), Soil erosion and carbon dynamics, *Soil Tillage Res.*, *81*, 137–142, doi:10.1016/j.still.2004.09.002.
Ludwig, J. A., P. Bradford, D. D. Breshears, D. J. Tongway, and A. C. Imeson (2005), Vegetation patches and runoff-erosion as interacting ecohydrological processes in semiarid landscapes, *Ecology*, *86*(2), 288–297, doi:10.1890/03-0569.
Marschner, B., et al. (2008), How relevant is recalcitrance for the stabilization of organic matter in soils?, *J. Plant Nutr. Soil Sci.*, *171*(1), 91–110, doi:10.1002/jpln.200700049.
Mayor, Á. G., S. Bautista, E. E. Small, M. Dixon, and J. Bellot (2008), Measurement of the connectivity of runoff source areas as determined by vegetation pattern and topography: A tool for assessing potential water and soil losses in drylands, *Water Resour. Res.*, *44*, W10423, doi:10.1029/2007WR006367.
Mendez-Millan, M., T. T. Nguyen Tu, J. Balesdent, S. Derenne, D. Derrien, C. Egasse, A. Thongo M'Bou, B. Zeller, and C. Hatté (2013), Compound-specific 13C and 14C measurements improve the understanding of soil organic matter dynamics, *Biogeochemistry*, 1–19, doi:10.1007/s10533-013-9920-7.
Mielnick, P., W. A. Dugas, K. Mitchell, and K. Havstad (2005), Long-term measurements of $CO_2$ flux and evapotranspiration in a Chihuahuan desert grassland, *J. Arid Environ.*, *60*, 423–436, doi:10.1016/j.jaridenv.2004.06.001.
Mukundan, R., D. E. Walling, A. C. Gellis, M. C. Slattery, and D. E. Radcliffe (2012), Sediment source fingerprinting: Transforming from a research tool to a management tool, *J. Am. Water Resour. Assoc.*, *48*(6), 1241–1257, doi:10.1111/j.1752-1688.2012.00685.x.
Muldavin, E., D. Moore, S. Collins, K. Wetherill, and D. Lightfoot (2008), Aboveground net primary production dynamics in a northern Chihuahuan Desert ecosystem, *Oecologia*, *155*(1), 123–132, doi:10.1007/s00442-007-0880-2.
Nadeu, E., A. A. Berhe, J. de Vente, and C. Boix-Fayos (2012), Erosion, deposition and replacement of soil organic carbon in Mediterranean catchments: A geomorphological, isotopic and land use change approach, *Biogeosciences*, *9*(3), 1099–1111, doi:10.5194/bg-9-1099-2012.
Okin, G. S., P. D'Odorico, and S. R. Archer (2009), Impact of feedbacks on Chihuahuan desert grasslands: Transience and metastability, *J. Geophys. Res.*, *114*, G01004, doi:10.1029/2008JG000833.
Olderman, L. R. (1994), The global extent of soil degradation, in *Soil Resilience and Sustainable Land Use*, edited by D. J. Greenland and I. Szabolcs, pp. 99–118, CAB International, Wallingford, U. K.
Parsons, A. J., A. D. Abrahams, and J. Wainright (1996), Responses of interrill runoff and erosion rates to vegetation change in southern Arizona, *Geomorphology*, *14*, 311–317, doi:10.1016/0169-555X(95)00044-6.
Parsons, A. J., R. E. Brazier, J. Wainwright, and D. M. Powell (2006), Scale relationships in hillslope runoff and erosion, *Earth Surf. Processes Landforms*, *31*(11), 1384–1393.
Peters, D. P. C., and J. E. Herrick (2001), Modelling vegetation change and land degradation in semiarid and arid ecosystems: An integrated hierarchical approach, *Adv. Environ. Monit. Model.*, *2*(1), 1–29.
Peters, D. P. C., W. Schlesinger, J. E. Herrick, L. Huenneke, and K. Havstad (2006), Future directions in Jornada research: Applying an interactive landscape model to solve problems, in *Structure and Function of a Chihuahuan Desert Ecosystem: The Jornada Basin Long-Term Ecological Research Site*, edited by K. M. Havstad, L. Huenneke, and W. H. Schlesinger, chap. 18, pp. 369–386, Oxford Univ. Press, New York.
Peters, D. P. C., et al. (2013), 4.20 - Desertification of rangelands, in *Vulnerability of Ecosystems to Climate*, edited by R. Pielke, pp. 239–258, Academic Press, Oxford, U. K., doi:10.1016/B978-0-12-384703-4.00426-3
Pierson, F. B., C. J. Williams, P. R. Kormos, S. P. Hardegree, P. E. Clark, and B. M. Rau (2010), Hydrologic vulnerability of sagebrush steppe following pinyon and juniper encroachment, *Rangel. Ecol. Manage.*, *63*(6), 614–629, doi:10.2111/rem-d-09-00148.1.
Poulter, B., et al. (2014), Contribution of semi-arid ecosystems to interannual variability of the global carbon cycle, *Nature*, *509*(7502), 600–603, doi:10.1038/nature13376.
Puttock, A., J. A. J. Dungait, R. Bol, E. R. Dixon, C. J. A. Macleod, and R. E. Brazier (2012), Stable carbon isotope analysis of fluvial sediment fluxes over two contrasting $C_4$-$C_3$ semi-arid vegetation transitions, *Rapid Commun. Mass Spectrom.*, *26*(20), 2386–2392, doi:10.1002/rcm.6257.
Puttock, A., C. J. A. Macleod, R. Bol, P. Sessford, J. Dungait, and R. E. Brazier (2013), Changes in ecosystem structure, function and hydrological connectivity control water, soil and carbon losses in semi-arid grass to woody vegetation transitions, *Earth Surf. Processes Landforms*, *38*(13), 1602–1611, doi:10.1002/esp.3455.
Ravi, S., D. D. Breshears, T. E. Huxman, and P. D'Odorico (2010), Land degradation in drylands: Interactions among hydrological and aeolian erosion and vegetation dynamics, *Geomorphology*, *116*(3–4), 236–245, doi:10.1016/j.geomorph.2009.11.023.
Rawling, G. C. (2004), *Geology and hydrologic setting of springs and seeps on the Sevilleta National Wildlife Refuge*, New Mexico Tech Report, Socorro.
Reid, K. D., B. P. Wilcox, D. D. Breshears, and L. MacDonald (1999), Runoff and erosion in a pinon-juniper woodland: Influence of vegetation patches, *Soil Sci. Soc. Am. J.*, *63*, 1869–1879, doi:10.2136/sssaj1999.6361869x.
Reynolds, J. F., et al. (2007), Scientific concepts for an integrated analysis of desertification, *Land Degrad. Dev.*, *22*(2), 166–183, doi:10.1002/ldr.1104.
Ridolfi, L., F. Laio, and P. D'Odorico (2008), Fertility island formation and evolution in dryland ecosystems, *Ecol. Soc.*, *13*(1), 5.
Schimel, D. S. (2010), Drylands in the Earth system, *Science*, *327*(5964), 418–419, doi:10.1126/science.1184946.
Schlesinger, W. H., J. F. Reynolds, G. L. Cunningham, L. F. Huenneke, W. M. Jarrell, R. A. Virginia, and W. G. Whitford (1990), Biological feedbacks in global desertification, *Science*, *247*, 1043–1048, doi:10.1126/science.247.4946.1043.

Schlesinger, W. H., T. J. Ward, and J. Anderson (2000), Nutrient losses in runoff from grassland and shrubland habitats in southern New Mexico: II. Field plots, *Biogeochemistry*, *49*(1), 69–86, doi:10.1007/BF00992871.

Seager, R., et al. (2007), Model projections of an imminent transition to a more arid climate in southwestern North America, *Science*, *316*, 1181–1184, doi:10.1126/science.1139601.

Sevilleta LTER (2014), Sevilleta long term ecological research: Where edges meet, 05.01. [Available at http://sev.lternet.edu/, (Accessed 27 July.]

Throop, H. L., and S. R. Archer (2008), Shrub (Prosopis velutina) encroachment in a semidesert grassland: Spatial–temporal changes in soil organic carbon and nitrogen pools, *Global Change Biol.*, *14*(10), 2420–2431, doi:10.1111/j.1365-2486.2008.01650.x.

Turnbull, L., J. Wainright, and R. E. Brazier (2008a), A conceptual framework for understanding semi-arid land degradation: Ecohydrological interactions across multiple-space and time scales, *Ecohydrology*, *1*, 23–34, doi:10.1002/eco.4.

Turnbull, L., R. E. Brazier, J. Wainwright, L. Dixon, and R. Bol (2008b), Use of carbon isotope analysis to understand semi-arid erosion dynamics and long-term semi-arid land degradation, *Rapid Commun. Mass Spectrom.*, *22*, 1697, doi:10.1002/rcm.3514.

Turnbull, L., J. Wainwright, and R. E. Brazier (2010a), Changes in hydrology and erosion over a transition from grassland to shrubland, *Hydrol. Processes*, *24*, 393–414, doi:10.1002/hyp.7491.

Turnbull, L., J. Wainwright, and R. E. Brazier (2010b), Hydrology, erosion and nutrient transfers over a transition from semi-arid grassland to shrubland in the South-Western USA: A modelling assessment, *J. Hydrol.*, *388*(4), 258–272, doi:10.1016/j.jhydrol.2010.05.005.

Turner, D. P., et al. (2005), Site-level evaluation of satellite-based global terrestrial gross primary production and net primary production monitoring, *Global Change Biol.*, *11*, doi:10.1111/j.1365-2486.2005.00936.x.

U.S. Fish and Wildlife Service (2014), [Available at http://www.fws.gov/refuge/Sevilleta/, Accessed 27 July 2014.]

U.S. Department of Agriculture, Soil Survey (2014), Soil Survey Staff, Natural Resources Conservation Service, United States Department of Agriculture, Web Soil Survey. [Available at http://websoilsurvey.nrcs.usda.gov/, Accessed 27th July 2014.]

Van Auken, O. W. (2009), Causes and consequences of woody plant encroachment into western North American grasslands, *J. Environ. Manage.*, *90*, 2931–2942, doi:10.1016/j.jenvman.2009.04.023.

Van Bergen, P. F., C. J. Nott, I. D. Bull, P. R. Poulton, and R. P. Evershed (1998), Organic geochemical studies of soils from the Rothamsted Classical Experiments-IV. Preliminary results from a study of the effect of soil pH on organic matter decay, *Org. Geochem.*, *29*(5–7), 1779–1795, doi:10.1016/S0146-6380(98)00188-0.

Van Oost, K., et al. (2007), The impact of agricultural soil erosion on the global carbon cycle, *Science*, *318*(5850), 626–629, doi:10.1126/science.1145724.

Wainwright, J., A. J. Parsons, and A. D. Abrahams (2000), Plot-scale studies of vegetation, overland flow and erosion interactions: Case studies from Arizona and New Mexico, *Hydrol. Processes*, *14*, 2921–2943, doi:10.1002/1099-1085(200011/12)14:16/17<2921::AID-HYP127>3.0.CO;2-7.

Wainwright, J., L. Turnbull, T. G. Ibrahim, I. Lexartza-Artza, S. F. Thornton, and R. E. Brazier (2011), Linking environmental regimes, space and time: Interpretations of structural and functional connectivity, *Geomorphology*, *126*, 387–404, doi:10.1016/j.geomorph.2010.07.027.

Wilcox, B. P., D. D. Breshears, and C. D. Allen (2003a), Ecohydrology of a resource-conserving semiarid woodland: Effects of scaling and disturbance, *Ecol. Monogr.*, *73*, 223–239, doi:10.1890/0012-9615(2003)073[0223:EOARSW]2.0.CO;2.

Wilcox, B. P., D. D. Breshears, and H. J. Turin (2003b), Hydraulic conductivity in a pinon-juniper woodland: Influence of vegetation, *Soil Sci. Soc. Am. J.*, *67*, 1243–1249, doi:10.2136/sssaj2003.1243.

World Resources Institute (WRI) (2002), Drylands, People, and Ecosystem Goods and Services: A Web-based Geospatial Analysis. [Available at http://www.wri.org.]

Wu, Y., J. Zhang, S. M. Liu, Z. F. Zhang, Q. Z. Yao, G. H. Hong, and L. Cooper (2007), Sources and distribution of carbon within the Yangtze River system, *Estuarine Coastal Shelf Sci.*, *71*(12), 13–25, doi:10.1016/j.ecss.2006.08.016.

Yu, K., and P. D'Odorico (2014), An ecohydrological framework for grass displacement by woody plants in savannas, *J. Geophys. Res. Biogeosci.*, *119*, 192–206, doi:10.1002/2013JG002577.

Zafar, A., U. Safriel, D. Niemeijer, R. White, and I. Press (2005), *Millennium Ecosystem Assessment, Ecosystems and Human Well-being: Desertification Synthesis*, Washington, D. C.

Zech, M., R. Zech, H. Morras, L. Moretti, B. Glaser, and W. Zech (2009), Late Quaternary environmental changes in Misiones, subtropical NE Argentina, deduced from multi-proxy geochemical analyses in a palaeosol-sediment sequence, *Quat. Int.*, *196*, 121–136, doi:10.1016/j.quaint.2008.06.006.